

lations is to show a concentration independent of height or decreasing somewhat at lower altitudes. This behavior is characteristic of a source at the top and a sink at the bottom, with downward flow by mixing and by gravitational settling. It seems to follow that there is a source of sulfur and  $\text{H}_2\text{SO}_4$  at or above 57 km, the top of the middle cloud region. The source is presumably photochemical in nature, requiring ultraviolet radiation that does not penetrate far into the sulfur cloud.

We suggest the following working interpretation of the middle and lower clouds and the lower haze. The large sulfur particles created near 57 km are slowly descending. As they reach the region of 51 km, they begin to evaporate, and near 48 km the residues melt to form the particles of the lower haze. The slow evaporation of these particles is a problem; perhaps it is retarded by the presence of sulfur vapor, or perhaps we are seeing the residue of a recent local shower. The large particles ( $> 30 \mu\text{m}$ ) observed in the middle and lower cloud layers are nearing mist sizes and would double their size by coalescence, falling through the 49- to 51-km layer. There is every reason to believe precipitation sizes could be produced in these clouds.

The  $\text{H}_2\text{SO}_4$  droplets (peak  $3.5 \mu\text{m}$ ) present from 56 to 51 km appear traceable into the lower cloud region. The modal size decreases somewhat toward the bottom of the middle cloud region, and then it largely disappears while a large size mode (of similar concentration) rapidly increases in the lower cloud region. This appears consistent with  $\text{H}_2\text{SO}_4$  droplets, which first lose water on the way down but then encounter increased  $\text{H}_2\text{O}$  (and perhaps  $\text{SO}_2$  and  $\text{SO}_3$ ) growing to form the lower cloud region of dilute acid and the densest layer. This layer must incorporate some of the 0.2 percent of water vapor observed at lower altitudes by the large probe gas chromatograph (6). Its base is the dominant planetary feature at the several planetary locations observed by the Pioneer Venus nephelometer (7) as well as by the Soviet nephelometer aboard Venera 9 and 10 (8).

It is clear that the Venus cloud system is far more complicated than we expected. Both  $\text{H}_2\text{SO}_4$  and sulfur particles seem identifiable, but other particles must be explained (for example,  $1\text{-}\mu\text{m}$  particles at 51 to 56 km). The Venus clouds are quite tenuous at certain altitudes, but because of the vertical extent, the total cloud optical depth integrates to more than 32 (and should increase to 36 to 40 when all data is received) and the

particle mass is equivalent to 0.1 to 0.2 mm of precipitation. Most importantly, the large sizes ( $> 10 \mu\text{m}$ ) encourage the possibility of precipitation on Venus, either in the dilute  $\text{H}_2\text{SO}_4$  lower cloud region or initiated by sulfur from the middle cloud region, which would pick up the dilute  $\text{H}_2\text{SO}_4$  when falling below 51 km. The significance of these large particles in returning mass downward cannot be overemphasized.

ROBERT G. KNOLLENBERG  
*Particle Measuring Systems, Inc.,*  
*Boulder, Colorado 80301*

D. M. HUNTEN  
*University of Arizona,*  
*Tucson 85724*

#### References and Notes

1. R. G. Knollenberg, *Proceedings of the International Cloud Physics Conference* (American Meteorological Society, Boston, 1976), pp. 554-561.
2. L. Colin, *Space Sci. Rev.* **20**, 249 (1977).
3. A. T. Young, *Icarus* **32**, 1 (1977); B. Hapke and R. Nelson, *J. Atmos. Sci.* **32**, 1212 (1975).
4. A. T. Young, *Icarus* **18**, 564 (1973); J. B. Pollack *et al.*, *ibid.* **23**, 8 (1974).
5. J. E. Hansen and J. W. Hovenier, *J. Atmos. Sci.* **31**, 1137 (1974).
6. V. I. Oyama, G. C. Carle, F. Woeller, J. B. Pollack, *Science* **203**, 802 (1979).
7. B. Ragert and J. Blamont, *ibid.*, p. 790.
8. M. Ya. Marov, V. N. Lebedev, V. E. Lysteev, I. S. Kuznetsov, G. K. Popandopulo, paper presented at the 19th meeting of the Committee on Space Research (of the International Council of Scientific Unions), Philadelphia, 14 to 19 June 1976.
9. We thank Ball Brothers Research Corporation, Boulder, Colo., for building the excellent LCPS instrument.

16 January 1979

## Preliminary Results of the Solar Flux Radiometer Experiment Aboard the Pioneer Venus Multiprobe Mission

**Abstract.** *The solar flux radiometer aboard the Pioneer Venus large probe operated successfully during its descent through the atmosphere of Venus. Upward, downward, and net fluxes from 0.4 to 1.0 micrometers were obtained at more than 390 levels between 185 millibars (at an altitude of ~61 kilometers) and the surface. Fluxes from 0.4 to 1.8 micrometers were also obtained between 185 millibars and about the level at which the pressure was 2 atmospheres. Data from 80 to 185 millibars should be available after additional decoding by the Deep Space Network. Upward and downward intensities in a narrower band from 0.59 to 0.66 micrometers were also obtained throughout the descent in order to constrain cloud properties. The measurements indicate three cloud regions above the 1.3-atmosphere level (at an altitude of ~49 kilometers) and a clear atmosphere beneath that level. At the 67° solar zenith of the probe entry site, some 15 watts per square meter are absorbed at the surface by a dark ground, which implies that about 2 percent of the solar energy incident on the planet is absorbed at the ground.*

Although Venus resembles Earth in size, mass, and distance from the sun, conditions at its surface are completely different from those at the surface of Earth. In particular, a remarkably high surface temperature near 750 K has been measured by several techniques. It is generally assumed that absorbed sunlight provides the energy that maintains the high surface temperature of Venus despite the planet's complete coverage by a highly reflective cloud layer. An understanding of the thermal balance of Venus requires a detailed knowledge of the amount of sunlight absorbed at various levels in its atmosphere and at the planet's surface. The planned contributions of the Pioneer Venus mission in this and other areas affecting the thermal balance have been outlined previously (1).

To obtain measurements of solar flux near the cloud tops where the sun is still visible from a spinning probe suspended beneath a parachute, the measurement scheme adopted used narrow fields of view ( $5^\circ$  full width at half maximum re-

sponse). When the sun was visible, the instrument determined the spin period of the probe and sampled the radiation field at known azimuth angles relative to the sun. When the sun was no longer directly visible (at optical depths greater than about 7 at the entry site), the instrument sampled as rapidly as the data rate allowed (every 8 seconds). Each measurement set contains data in two broad spectral channels, from 0.4 to  $1.0 \mu\text{m}$  and from  $1.0$  to  $1.8 \mu\text{m}$ , in three upward-looking directions at angles of  $27^\circ$ ,  $60^\circ$ , and  $83^\circ$  from the zenith and two downward-looking directions at angles of  $102^\circ$  and  $142^\circ$  from the zenith. In addition, data were collected in a narrower spectral channel from  $0.59$  to  $0.66 \mu\text{m}$  at zenith angles of  $60^\circ$  and  $142^\circ$  (Fig. 1). Thus, except near the cloud tops where azimuthal information was obtained, the data consist of sets of 12 intensity samples obtained at 8-second intervals during the descent. The broad-band upward-looking samples are used in a three-point Gaussian quadrature for the downward flux, and the downward-looking chan-

nels form a separate two-point Gaussian quadrature for the upward flux. [When azimuthal information was present, the azimuth samples were first combined in a separate Gaussian quadrature for the azimuth integral of the intensity; see (2) for the locations of the samples.] The difference between the downward and upward flux gives the net flux at each measurement level, and the differences between the net fluxes at various levels gives the solar energy absorbed by the atmosphere between those levels. The narrow-band intensities were not used for the flux calculations but provide additional information on the distribution and optical properties of the clouds throughout the descent.

The main advantage of the sampling scheme is that it allows the determination of fluxes at small optical depths even in the presence of the parachute and the spinning probe. In addition, it gives information on the azimuthal structure of the radiation field near the cloud tops and thus helps to constrain the optical

properties of the cloud particles there. Also, the use of more than one sample in both the upward and downward hemispheres provides for consistency checks and some measure of redundancy in case of instrument problems. A summary of the solar flux radiometer (LSFR) instrument characteristics has been given by Colin and Hunten (2).

The LSFR seems to have operated as planned throughout its descent to the surface of Venus. The instrumental goals that were successfully accomplished and that are necessary for reliable flux information include the following.

An extensive and consistent set of dark current data was obtained during the period just before entry. Further, the in-flight calibration of the LSFR logarithmic amplifiers using calibration currents superimposed on signal currents at 2-minute intervals throughout the descent indicated no significant change in the properties of the LSFR electronics since prelaunch calibration.

The temperatures of the detector array

and of the electronics package varied smoothly and as anticipated throughout the descent. The phase change material limited the detector temperature to less than 45°C throughout the descent.

The azimuth sampling logic appears to have worked correctly. Because of the complex procedures used by the Deep Space Network to decode the first few minutes of the telemetry stream after entry, these data are not yet available. Nevertheless, the engineering data beginning at the pressure level of about 185 mbar indicate that the sun was visible at parachute deployment (roughly 80 mbar of pressure) and that the level at an optical depth of 7 was crossed somewhere between the 80- and 185-mbar pressure levels. Thus, when all of the data are decoded, we should obtain fluxes to quite small optical depths.

Even more important, the radiation field at pressure levels from 185 mbar to the surface showed no discernible azimuthal patchiness. This fact greatly simplifies the conversion of our intensity samples to fluxes.

The dependence of the radiation field on zenith angle is about as expected (nearly linear in the cosine of the zenith angle), and preliminary data indicate no significant problems resulting from cloud particles or other contaminants on our windows.

When an average responsivity is defined for both the 0.4- to 1.0- $\mu\text{m}$  channel and the combination of the two broad channels (Fig. 1), the signal currents can be converted to intensities and then to upward, downward, and net fluxes in a straightforward way (Fig. 2). The deviations from flatness of our spectral response can be expected to introduce some error in the derived intensities and fluxes. Nonetheless, our experience in modeling the spectrum of the radiation field in the atmosphere of Venus indicates that the error is about 10 percent or less for the net flux in 0.4- to 1.0- $\mu\text{m}$  region and even less for the next flux between 0.4 and 1.8  $\mu\text{m}$ , derived by adding the signals from the two broad channels and using the average value of the sum of the responsivities of the silicon and germanium channels. The limiting accuracy on the net fluxes likely results instead from the degree to which the responsivities of the upward- and downward-looking channels are known relative to each other. High in the clouds, the upward flux is only about 10 percent less than the downward flux. Thus, errors of 2 percent of the opposite sign in the upward and downward channels would result in a 40 percent error in the net flux.

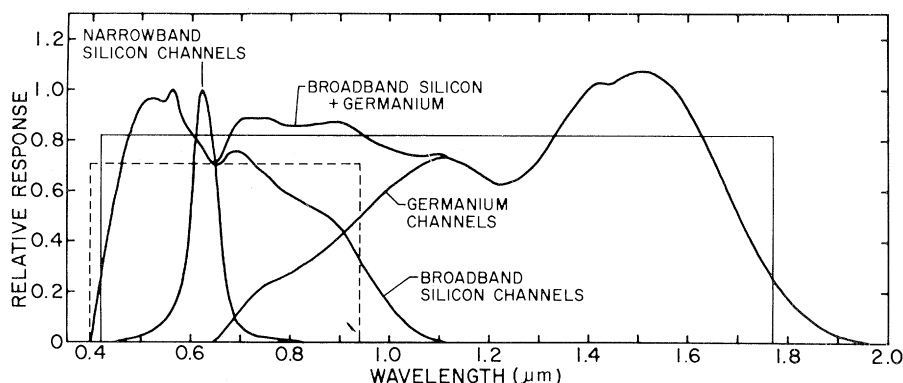
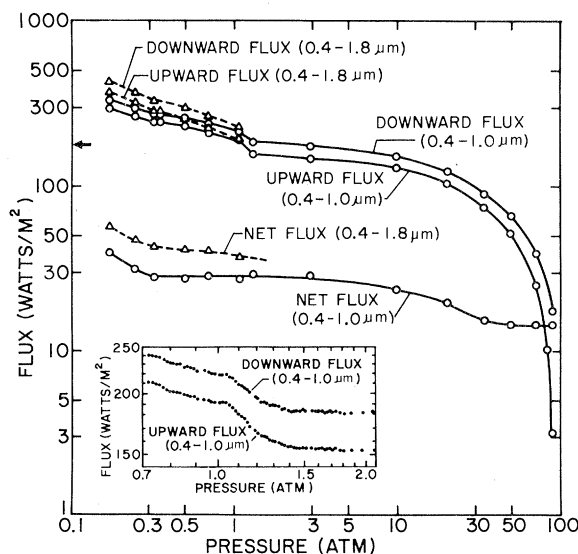


Fig. 1. The relative spectral response of the LSFR spectral channels versus wavelength. The broad-band silicon and the combination of the broad-band silicon plus germanium channels were approximated by the rectangles shown for the derivation of the fluxes given in Fig. 2.

Fig. 2. The upward, downward, and net fluxes versus pressure for the spectral intervals given. The conversion from time to pressure is from Seiff (6). For reference, the approximate net flux value at the top of the atmosphere at the probe entry site is marked by the arrow. The insert shows the full vertical resolution of the data in the region around the cloud bottom. Note the good agreement between features in the upward and downward fluxes (which were measured by different detectors and amplifiers), which indicates that statistical errors are small. Evidence for three cloud layers is seen in the slope changes at about 0.32, 1.03, and 1.3 atm.



At lower levels, when the percentage difference between the upward and downward flux becomes much larger, the net flux becomes easier to measure. Near the surface, the ratio between upward and downward flux approaches 6, and the net flux is essentially known to the accuracy of the downward flux alone. At present, we believe that the individual fluxes are known to an absolute accuracy of about 15 percent and that the upward and downward fluxes are each known relative to each other to about  $\pm 2$  percent.

Together, the three sources of uncertainty in absolute response, relative response, and nonflat spectral response probably result in less than 20 percent uncertainty in the net flux near the surface and less than 40 percent uncertainty at high altitudes. The systematic uncertainties affect the net flux profile in predictable ways. Because the statistical noise in the data is small, the features in the curve are well established. As we continue to refine the calibration and particularly as the data at the highest altitudes become available and are tied to ground-based and orbiter data from outside the atmosphere, these uncertainties should be reduced.

Several interesting features are apparent in Fig. 2. At pressures greater than 1.3 atm, the variation of upward and downward flux with depth is very smooth and slow in contrast to the situation at lower pressures. Detailed inspection of the low-pressure region indicates excellent correlation of the rate of flux decrease with the measurement of cloud layers by the cloud particle size spectrometer (3) and the nephelometer experiments (4). In particular, three different rates of flux decrease are seen between 1.03 and 1.3 atm, 0.32 and 0.97 atm, and less than 0.32 atm. The clouds at pressures greater than 0.32 atm absorb remarkably little sunlight.

The flux profiles at pressures greater than 1.3 atm are consistent with that expected for a Rayleigh scattering atmosphere with a small amount of absorption. The upward and downward fluxes are very different at our lowest measurement levels, implying a ground albedo less than about 15 percent in the visible.

The solar constant at Venus of about 2600 W/m<sup>2</sup> implies a downward solar flux incident at the top of the atmosphere at the entry site ( $\sim 67^\circ$  solar zenith angle) of about 1000 W/m<sup>2</sup>. Model calculations we have made that are consistent with the spherical albedo of Venus give a bolometric net solar flux at the top of the atmosphere of roughly 180 W/m<sup>2</sup> at this so-

lar zenith angle. About half of this 180 W/m<sup>2</sup> is absorbed above the 185-mbar level. Fig. 2 gives the net flux profile below this level for the wavelength regions shown. About 15 W/m<sup>2</sup> in the 0.4- to 1.0- $\mu$ m region are absorbed at the ground. We calculate that the planet-wide average flux profile is about 20 percent less than the flux profile measured at  $67^\circ$  solar zenith angle. Averaged over the entire planet, some 12 W/m<sup>2</sup> are absorbed at the ground. The fraction of the incident solar energy that is absorbed at the ground is thus about  $(4\pi R_v^2 \times 12 \text{ W/m}^2)/(\pi R_v^2 \times 2600 \text{ W/m}^2)$ , or about 2 percent.

Accurate measurement of the solar energy deposition profile provides data essential for determining the effectiveness of the greenhouse mechanism. Although we have not yet completed detailed calculations based on these measurements, some evidence already exists that the greenhouse mechanism will support a high surface temperature. Calculations by Pollack and Young (5) based on Venera data in which some 1 percent of the incident sunlight reached the ground have been able to give high surface temperatures for some assumption of thermal opacity. These measurements should allow the greenhouse to work even with slightly lower thermal opacity.

In addition to further work to refine our instrumental calibration, we plan theoretical studies in three areas. First, we intend to model the angular distribution of the measured intensities for a wide

range of optical properties in the clouds. We hope to derive not only the optical depths of the cloud layers but also the single scattering albedos and phase functions of the cloud particles. Second, we plan to continue our model calculations of solar deposition at a variety of solar zenith angles to refine the factors used to scale our measurements to planet-wide averages. Finally, we have begun a series of globally averaged greenhouse model calculations to investigate the temperature profiles that our net flux profiles imply for various sources of thermal opacity.

M. G. TOMASKO, L. R. DOOSE  
J. PALMER, A. HOLMES  
W. WOLFE, N. D. CASTILLO  
P. H. SMITH

*Lunar and Planetary Laboratory  
and Optical Science Center,  
University of Arizona, Tucson 85721*

#### References and Notes

1. M. G. Tomasko *et al.* *Space Sci. Rev.* **20**, 389 (1977).
2. L. Colin and D. M. Hunten, *ibid.*, p. 468.
3. R. G. Knollenberg and D. M. Hunten, *Science*, **203**, 792 (1979).
4. B. Ragert and J. Blamont, *ibid.*, p. 790.
5. J. B. Pollack and R. Young, *J. Atmos. Sci.* **32**, 1025 (1975).
6. A. Seiff (1978), personal communication.
7. We are especially indebted to several individuals for the success of this experiment, including the late Dr. A. E. Clements for his many contributions to the original design of the experiment; L. Thane and K. Schlichtemeyer of the Martin Marietta Corporation for the outstanding performance of the LSFR electronics; and J. Ferandin and his colleagues at NASA-Ames Research Center for delivering a data tape so rapidly after Venus entry.

16 January 1979

## First Results from the Large Probe Infrared Radiometer Experiment

**Abstract.** *During the descent to the surface of Venus, the large probe infrared radiometer measured the net thermal radiative flux in several spectral bandpasses. Preliminary analysis has permitted us to estimate (i) the infrared extinction coefficient profile attributable to aerosols, with respect to their visible profile, in the upper atmosphere of Venus and (ii) the water vapor mixing ratio below the clouds. An indication of the composition of a multicomponent cloud is seen in the data from the spectral bandpass from 6 to 7 micrometers.*

The objectives of the large probe infrared radiometer (LIR) experiment were to measure the net thermal flux and its divergence, to detect clouds and determine their infrared opacity, and to detect the presence of water vapor (and obtain an estimate of its abundance) during descent through the atmosphere of Venus. The instrument is a multichannel infrared radiometer that alternately measures the upward and downward radiation. The difference between these measurements, the net flux, constitutes

the data that were transmitted to Earth. Descriptions of the hardware have been published elsewhere (1, 2). The nominal spectral bandpasses used were (i) for the net thermal flux, 3 to 150  $\mu$ m, (ii) for cloud detection, 8 to 9  $\mu$ m (a CO<sub>2</sub> "window"), and (iii) for water vapor, 6 to 7 and 7 to 8  $\mu$ m.

At the present state of data reduction all indications are that the instrument itself functioned correctly throughout the mission. Tests covering the periods before the launch, during the cruise, and